LA-UR-17-25251
Approved for public release; distribution is unlimited.

Title: Calibration and Propagation of Uncertainty for Independence

Author(s): Holland, Troy Michael
Kress, Joel David
Bhat, Kabekode Ghanasham

Intended for: Report

Issued: 2017-06-30

Calibration and Propagation of Uncertainty for Independence

Troy Holland
Joel D. Kress
K. Sham Bhat
Los Alamos National Laboratory

and

Ye Yuan
Gary T. Rochelle
University of Texas at Austin

Prepared for
U.S. Department of Energy
National Energy Technology Laboratory

5/30/2017

Revision Log

Revision	Date	Revised By:	Description
0	5/30/2017	Joel D. Kress	Original

Disclaimer

Table of Contents

List of Figures

List of Tables

1.0 Executive Summary

This document reports on progress and methods for the calibration and uncertainty quantification of the Independence model developed at UT Austin. The Independence model is an advanced thermodynamic and process model framework for piperazine solutions as a high-performance CO_2 capture solvent. Progress is presented in the framework of the CCSI standard basic data model inference framework. Recent work has largely focused on the thermodynamic submodels of Independence.[1]

[1] This uncertainty quantification work constitutes of portion of a PhD. thesis currently in preparation. See 1.Holland, T. M. A Comprehensive Coal Conversion Model Extended to Oxy-coal Conditions. Brigham Young University, Provo, UT, 2017.

2.0 Milestone Summary and Completion

Milestone M1.17.2.3 objective: Update the Independence vapor-liquid equilibrium (VLE) thermodynamic basic data models. The Independence model is an advanced thermodynamic and process model framework for piperazine solutions as a high-performance CO_2 capture solvent. The submodels in the original Independence model were sequentially regressed set of parameters from numerous data sets in the Aspen Plus modeling framework. The data sets for preliminary uncertainty quantification and propagation are:

- Low temperature water/amine heat capacity data (Hilliard, 2008[2])
- High temperature water/amine heat capacity data (Nguyen, 2012[3])
- Water/amine volatility data (Hilliard, 2008[2] and Nguyen, 2012[3])
- Low temperature CO_2 solubility data (Dugas, 2009[4], and Fulks, 2011[5])
- High temperature CO_2 solubility data (Xu, 2011[6])
- Loaded CO_2 heat capacity (Freeman, 2010[7])

From the above data the Henry's constant ($H_{i,H2O}$), unloaded PZ/water asymmetric activity coefficient (γ_{pz}*), and solution heat capacity were regressed using a Gaussian process (GP) based emulation and calibration.

Scope

- Receive model and data
- Dissect model to establish theoretical motivations and parameters to be calibrated
- Determine physically feasible ranges and prior distributions on model parameters
- Determine observational error in the data to the extent possible
- Calibrate the model to available data
- Quantify uncertainty
- Suggest model updates based on calibrated model/data discrepancy

The CCSI UQ methodology was demonstrated for monoethanolamine (MEA) in a recent publication.[8] This methodology is consistently applied throughout CCSI, as evidenced by the piperazine work in the Independence frame-work reported here. Figure 1 below outlines the method employed in the recent publication and the direct parallels the current methodology applied at LANL. In this case, both systems are chemical solvent process models, and the details of the methodology are very highly analogous to each other in both the MEA and piperazine (PZ) systems. However, the same methodology can readily be adapted to numerous scenarios in virtually all disciplines. Note that the process model is initially developed from industry best-practices prior to any UQ or calibration. Subsequently, the next three steps break the process model down into submodels and identify model parameters. Where possible, subsets of data are used to calibrate individual submodels for a clean, simple calibration. The resulting posterior

distributions and model discrepancy may then be propagated forward into more complex or physically intertwined submodels. In the case of CO_2 capture solvents, it is difficult to isolate chemical kinetic parameters, hydraulic parameters, and mass transfer parameters from each other, so several submodels may be jointly calibrated to relevant data sets in an effort to find self-consistent parameter posteriors. Finally, the parameter posteriors and their discrepancy are propagated into the original process model and any additional process model parameters are calibrated (such as a packing efficiency coefficient). Ultimately, a statistical emulator or calibrated model will produce process model predictions. These predictions will differ from measured data, and the discrepancy function will offer insight at every level of the calibration into where and how physical models should be extended to more closely match reality. Critical data gaps may also be identified. In either case, it will often be useful to iterate on the UQ and calibration process as calibration results inspire updated models and additional data collection.

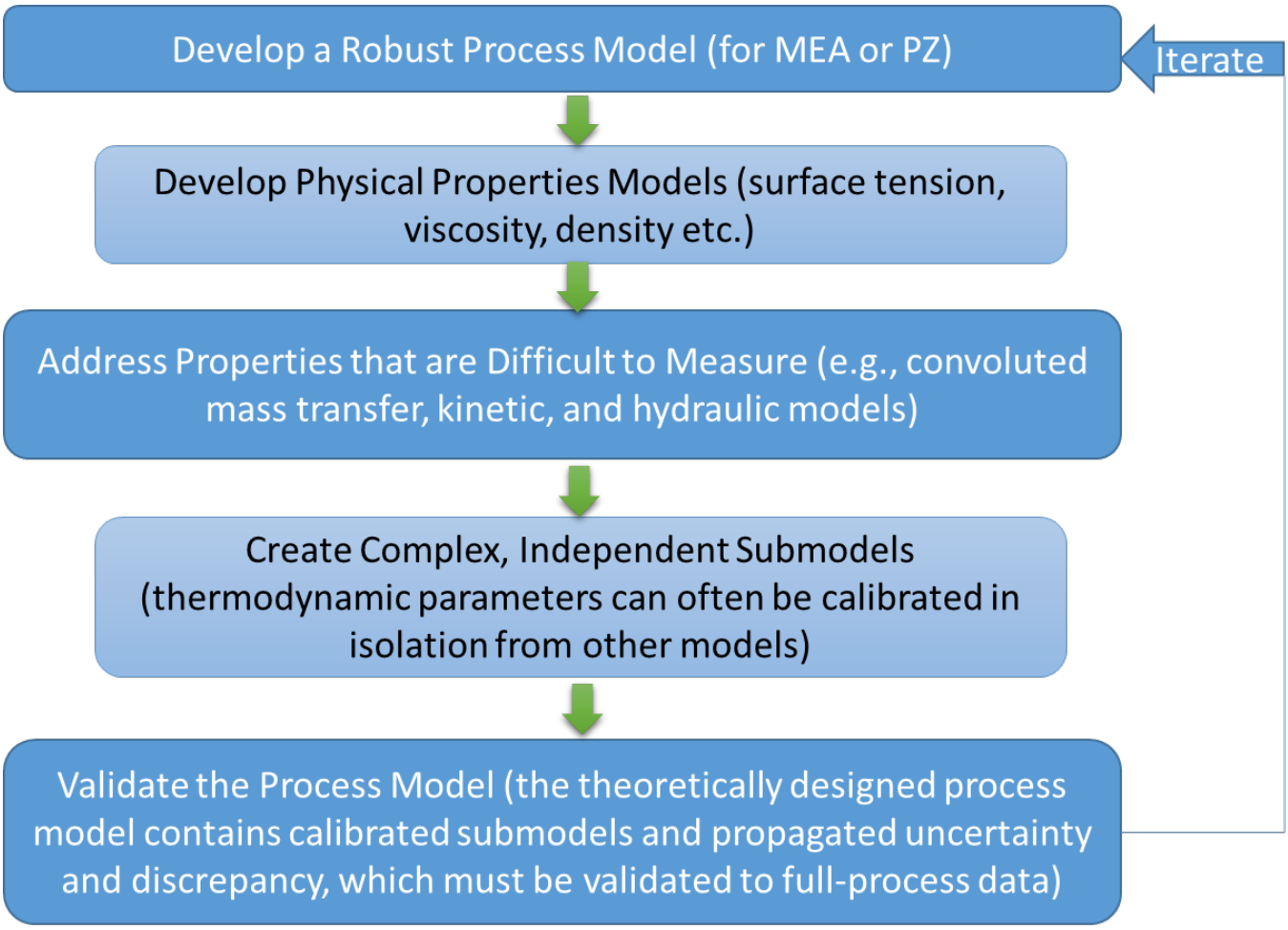

Figure 1 – A logic flow diagram for the CCSI UQ and calibration methodology. The methodology outlined here is suitable for any chemical process model, and can easily be generalized to a vast array of physical modelling scenarios.

3.0 Uncertainty Quantification and Calibration

Bayesian Calibration

Bayes' Law itself is an almost trivial statement of probability law, as seen in Equations 3-1 through 3-4. This derivation utilizes only the commutative property of probabilities and a definition of conditional probability. The result (Equation 3-4) is known as Bayes' Law, and the terms P(A|B), P(B|A), P(A), and P(B) are known respectively as the posterior, the likelihood, the prior of A and the prior of B. In discussions of model calibration, Bayes' Law is better couched in terms y (model output), **x** (model input), and **θ** (model parameters for both the physical model and the statistically machinery) as in Equation 3-5, where **θ** is the vector containing all model parameters (both for the physical model and the internal, statistical parameters).

$$P(A \cap B) = P(B \cap A) \quad 3\text{-}1$$

$$P(A \cap B) = P(A|B)P(B) \quad 3\text{-}2$$

$$P(A|B)P(B) = P(B|A)P(A) \quad 3\text{-}3$$

$$P(A|B) = \frac{P(B|A)P(A)}{P(B)} \quad 3\text{-}4$$

$$f_{\Theta|Y}(\mathbf{y}|\boldsymbol{\theta}) \propto f_{Y|\Theta}(\mathbf{y}|\boldsymbol{\theta}) f_{\Theta}(\boldsymbol{\theta}) \quad 3\text{-}5$$

Equation 3-5 merits considerable explanation. First, Equation 3-5 is composed of pdfs of the posterior, the likelihood, and the prior of **θ**, and omits the prior probability distribution of y. Second it is a proportionality, not strictly an equation. Note that the capital letters designate a random variable (i.e., the map between an event (with some pdf) and a corresponding numerical value) while the lower case letters indicating specific realizations or outcomes (a particular vector of parameter values (**θ**) or data points (y)). The following bullets detail the terms of Equation 3-5:

- The prior of y ($f_Y(y)$) is effectively a scaling factor that would constrain the left hand side probability distribution to integrate to unity (as required for a pdf). However, the prior of y physically corresponds to the pdf of the experimental data, which is not generally accessible. Fortunately, the calibration of a model searches for the most likely parameter values, given the data and prior beliefs regarding parameter values, so relative likelihood given any sets of parameters is retained, regardless of any scaling factor. Thus, knowledge of f_Y is not necessary for practical application.
- The prior of **θ** (f_Θ (**θ**)) physically represents prior beliefs on the joint pdf of every model parameter and every internal parameter. As a matter of practical convenience, the joint pdf is typically assumed to be uncorrelated, and each parameter effectively has its own pdf, which is often simply the uniform pdf over some range of physically feasible space as determined by a domain expert. In reality, the model form typically dictates some

correlation between model parameters, which should ideally be accounted for. The aforementioned internal parameters are those parameters that are necessary to execute the calibration, but not part of the mathematical model meant to capture some physical phenomenon. An example is given in Equation 3-6, where σ_i is an internal parameter; see the next bullet point for an explanation for Equation 3-6.

$$f_{Y|\Theta}(\mathbf{y}|\boldsymbol{\theta}) = \prod_{i}^{n} N(y_i; \mu_i(x), \sigma_i) \qquad 3\text{-}6$$

- The likelihood function ($f_{Y|\Theta}(\mathbf{y}|\boldsymbol{\theta})$) (in this case, Equation 3-6) is often the most difficult to compute from a practical standpoint. Physically, the function quantifies the question, "How likely are the data, given the numerical values of the current parameter vector $\boldsymbol{\theta}$?" In other words, if specific values are plugged into a model, how likely are those parameters to explain (or fit) the data. The answer to the goodness of fit question must include information about the noise or observational error in the data. Equation 3-6 quantifies the likelihood (and captures the observation error) with commonly employed assumptions: the data points are independent, so the probability of all observations is the product of the probability of each observation (the observation y_i has no bearing on the observation y_{i+1}), identically distributed (the observation error distribution is the same for all y_i), and normally distributed (fully defined by the normal pdf equation with some μ and σ). The parameter σ_i is an internal parameter if it cannot be reliably estimated from other information, which is to say it is necessary to compute the likelihood function, but is not known, and must be calibrated against the data along with the other parameters in $\boldsymbol{\theta}$. It represents the standard deviation of the normally distributed observation error for observation y_i, and if the errors are considered to be identically distributed, the value of σ_i is constant for all i. On the other hand, μ_i is typically formulated as a function of $\boldsymbol{\theta}$. When evaluating any vector of model parameters (a subset of vector $\boldsymbol{\theta}$), the model will predict a specific value given the values of vector $\boldsymbol{\theta}$ and the experimental inputs associated with data point y_i (the predicted value is then designated as μ_i). Since the goal is to evaluate the likelihood of the parameter values in $\boldsymbol{\theta}$ for the specific model in question, the output of model under the conditions of y_i with specific values of $\boldsymbol{\theta}$ is a reasonable mean. If the probability density ($N(y_i;\mu,\sigma)$) of y_i under conditions i with the specific values of $\boldsymbol{\theta}$ is very low, then the experimental value of y_i is several standard deviations away from the model prediction (the mean of the normal pdf), and the values of $\boldsymbol{\theta}$ do not result in a model that represents the data well. Note that if σ is considered an internal parameter to be calibrated, it requires a prior pdf. This prior is often not based on knowledge of the actual observational error (which is unknown, otherwise σ would have a fixed value). Instead, it is typically a prior that favors small values, under the assumption that the experiments resulted in reasonably consistent observations with pains taken to minimize error.
- Finally, the posterior pdf of the parameters given the data ($f_{\Theta|Y}$) is the product of the likelihood of the data given the parameters and the prior parameter probability. This can be calculated simultaneous or sequentially for multiple experiments or multiple data points in the same experiment. The result is the same, but the prior in the sequential case is the posterior of the immediately preceding data point (i.e., the prior of θ for point y_{i+1} is

the posterior for point y_i). The posterior is a joint pdf of dimensionality equal to the length of $\boldsymbol{\theta}$), and samples from the posterior can be inserted into the model to generate model predictions with quantified uncertainty, as in Equation 3-7, where $y_{p,i,j}$ is the predicted output for the conditions of data point i and using parameters from sample j, η is the model output (or emulator output) for the sample parameters and experimental inputs, and ε_i is the observational error. Numerous samples build what amounts to an error bar conditional on $\mathbf{x}_i$ and $\boldsymbol{\theta}_j$.

$$y_{p,i,j} = \eta(\mathbf{x_i}, \boldsymbol{\theta_j}) + \varepsilon_j \quad \text{3-7}$$

In addition, the calibration process may include some discrepancy term δ, which models the difference between reality and model predictions as a function of experimental inputs. Ideally, the model should be constructed to perfectly reflect reality, but in all practical applications this is not possible. As a simple example, ballistic motion can be captured by integrating the acceleration of an object with respect to time (one integration obtains the velocity equation, while two integrations yields the position equation). In many contexts, the integration neglects drag force as a matter of convenience, but this always introduces some error, which should be reflected in δ. In this case, δ would generally be small at small velocity values and large as high velocity increases the magnitude of drag forces. In general, the calibrated model would have some form as in Equation 3-8.

$$y_{p,i,j} = \eta(\mathbf{x_i}, \boldsymbol{\theta_j}) + \delta(\boldsymbol{x_i}) + \varepsilon_j \quad \text{3-8}$$

Gaussian Processes (GPs) for Model Emulation

In general, statistical model emulation seeks to capture the relationship between model inputs and outputs without requiring the computational expense of physical models. This allows a simulation scientist to explore expensive models in a timely manner, using relatively few runs from a high-cost computational experiment. Statistical surrogate models or emulators are especially useful in evaluating model predictions where no input/output pairs are given from the computational experiment. See Welch et al. [9] and Sacks et al. [10] for further discussion on the subject of statistical emulators. Gaussian processes are a popular and powerful tool for statistical emulation because they have the potential for enormous flexibility with relatively few parameters and they naturally incorporate uncertainty in model output. Gaussian processes are fully defined by a vector of mean values and a covariance matrix, so defining an emulator is conceptually as simple as arriving at the relevant mean and covariance. In some well-behaved cases, such as a linear model of p dimensions, the mean may be immediately obvious, and the covariance matrix can be generated from a kernel function. The kernel for a one-dimensional, linear covariance matrix for n data points on the domain $-1 \leq x \leq 1$ is shown in Equation 3-9, where $\mathbf{x}$ is the independent variable vector of length n, and i and j are used as indices in the covariance matrix.

$$Cov(i,j) = \mathrm{x}_i x_j \qquad 3\text{-}9$$

More complex cases require a more complex kernel or a covariance function tuned to the specific scenario and physical model. The model η is a statistical emulator (specifically a GP), and both δ and ε are similarly constructed GPs. The sum of the three GPs is also a GP, and an appropriate sample from the posterior distributions of **θ** in conjunction with any input values in the domain yields a model prediction including model and observational uncertainty as shown in Equation 3-8. The emulators for η, δ, and ε are fully defined by mean and covariance matrices as shown below. Further details are available elsewhere [11-14]. Equation 3-10 differs subtly from Equation 3-8 in that the model predictions for the i^{th} input and j^{th} sample of **θ** is not the prediction of interest. Instead, Equation 3-10 is an emulator that captures model behavior for the vector **x** for the i^{th} set of input conditions at some fixed vector **θ*** that includes the model parameters and the emulator internal parameters. GP emulators require internal parameters, which are represented in Equation 3-10 by IP. The emulator could also use samples from the posterior of **θ*** (the vector of parameters **and** internal parameters for η) to generate estimates of uncertainty, and $\eta(\mathbf{x},\boldsymbol{\theta})$, $\delta(\mathbf{x_i})$, and ε_i in Equation 3-8 may well be emulators, in which case Equations 3-8 and 3-10 are identical.

Gaussian Processes for Model Calibration

In principle, Bayesian calibration with GPs is identical to the Bayesian calibration with the simple model shown in Section 0, though the details of execution differ. In particular, the priors and hyper-priors of internal parameters becomes very complex, and the form of the likelihood function is far less neat.

GP calibration requires model parameters and prior distributions as inputs. In addition, internal parameters are required for the GP emulator to function as it explores the parameter space and generates a posterior distribution of the model parameters, model discrepancy, and observational uncertainty. The internal parameters are not fixed values; instead they each have their own prior distribution (called hyper-priors) which is adjusted during the calibration process.

Figure 2 summarizes the concepts of calibration and UQ from a graphical point of view. In Figure 2, the prior distributions on both **θ** and **IP** are informed by the data (the likelihood function is computed for both internal parameters and model parameters), and a new, posterior parameter space is produced, where parameter values that are likely to explain the data have a high probability density while parameter values that explain the data very poorly are assigned correspondingly low probability densities.

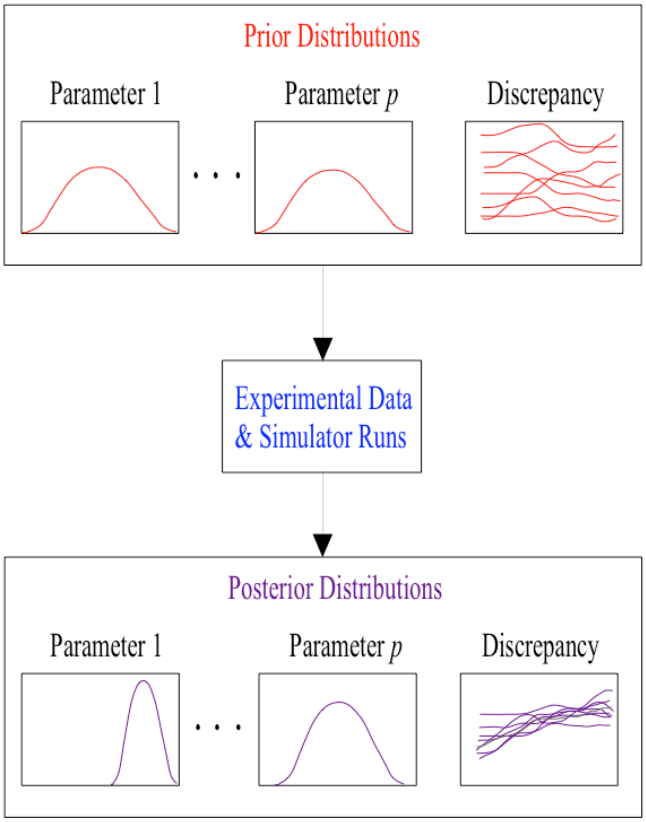

Figure 2 – Graphical representation of model calibration with discrepancy

As a final note, the likelihood function itself is not given here, both because it is extremely intricate and lengthy, and because any reader interested in that level of detail would do far better to thoroughly peruse the literature references in an effort to reconstruct highly advanced model analysis machinery.

Models

The UT Austin Piperazine model "Independence" is a collection of thermodynamic, kinetic, and heat and mass transfer submodel in the Aspen Plus framework. Some of the submodels are user models written in FORTRAN, but the majority are native Aspen submodels with user defined parameters. Ultimately, the uncertainty quantification (UQ) and calibration work will calibrate four layers of submodels: thermodynamics, kinetics, heat and mass transfer, and the full process model of a CO_2 absorber/stripper system. Further data and detailed descriptions are available elsewhere.[2-7] Because the submodels contain numerous parameters calibrated to a large body of data, it is mathematically and computationally unfeasible to simultaneously calibrate all parameters in all submodels. Instead, the strategy of sequential calibration with carefully propagated uncertainty between submodels has been adopted. The thermodynamic submodels and parameters have been identified and separately calibrated.

Non-Random Two Liquid Electrolyte Model (NRTLe)

The NRTLe model is an activity coefficient model native to Aspen plus with a number of internal parameters. It predicts activity coefficients based on molecular interactions in the liquid phase. The interactions fall into 3 categories (local, Pitzer-Debye-Huckle, and Born), and they are captured in the asymmetric Gibbs excess energy in Equation 3-1, where the asterisk indicates the asymmetric convention (i.e., the related activity coefficient is $\gamma^* = \gamma / \gamma^{\infty}$). Equation 3-2 show the relation between the asymmetric Gibbs excess energy and the asymmetric activity coefficient.

$$G_{Ex}^{*} = G_{Ex,lc}^{*} + G_{Ex,PDH}^{*} + G_{Ex,Born}^{*} \quad \textbf{3-10}$$

$$RT * ln(\gamma_i^{*}) = \frac{\partial G_{Ex}^{*}}{\partial n_i} \quad \textbf{3-11}$$

All three liquid interactions are represented by a number of complex expressions with numerous parameters. However, in this work, only the local contribution is considered for calibration and UQ, with other parameters being considered fixed in the present scope of work. The local Gibbs excess energy contribution is calculated via Equation 3-3, where m, c, and a denote molecule, cation, and anion respectively. The constituents of Equation 3-3 are given by Equations 3-4 through 3-7. Because α is set by a heuristic (0.3 for molecule-molecule interactions, 0.2 for electrolyte-electrolyte or molecule-electrolyte interactions where the molecule is water, and 0.1 where the molecule is a solute), only the values of various types of τ need to be computed. The value "G" (shown in Equation 3-6 for molecule-ionic pairs) represents differences in liquid component interaction that contribute to a non-ideal solution and thus a non-unity activity coefficient. Since the value of G is not often known, Equations 3-6 is used to compute it, which in turn requires an alternative approach to obtain τ. Equations 3-4, 3-5, and 3-7 are empirical correlations with (typically regressed) parameters that give τ as a function of temperature in K. Given the many pair-wise interactions in real systems, the total number of parameters to be regressed quickly becomes prohibitive, and often only the first one or two parameters in the empirical correlations are non-zero. See Table 3-1 for additional details on parameter equations and locations in Aspen Plus, and note that $X_j = x_j C_j$, where x is the mole fraction and C is either z (the charge on the ion) or unity for molecules.

$$\frac{G^{*}_{Ex,lc}}{RT} = \sum_m X_m \frac{\sum_j X_j G_{jm}\tau_{jm}}{\sum_k X_k G_{km}} + \sum_c X_c \sum_{a'}\left(\frac{X_{a'}}{\sum_{a''} X_{a''}}\right)\frac{\sum_j G_{jc,a'c}\tau_{jc,a'c}}{\sum_k X_k G_{jc,a'c}} + \sum_a X_a \sum_{c'}\left(\frac{X_{c'}}{\sum_{c''} X_{c''}}\right)\frac{\sum_j G_{ja,a'c}\tau_{ja,a'c}}{\sum_k X_k G_{ja,a'c}} \quad \textbf{3-12}$$

$$\tau_{mc,ac} = -ln\left[\sum_a \frac{X_a exp(-\alpha_{ca,m}\tau_{ca,m})}{\sum_{a'} X_{a'}}\right] - \tau_{ca,m} + \tau_{m,ca} \quad \textbf{3-13}$$

$$\tau_{m,ac} = A_{m,ac} + \frac{B_{m,ac}}{T} + C_{m,ac}\left(\frac{T^{ref}-T}{T} + ln\left(\frac{T}{T^{ref}}\right)\right) \quad \textbf{3-14}$$

$$G_{mc,ac} = exp(-\alpha_{ca,m}\tau_{mc,ac}) \quad \textbf{3-15}$$

$$\tau_{m,m'} = A_{m,m'} + \frac{B_{m,m'}}{T} + \cdots \quad \textbf{3-16}$$

In addition to the activity coefficient equations, the thermodynamic system in Independence requires self-consistency between submodels for Henry's constant, heat capacity, vapor-liquid equilibrium, and chemical equilibrium. The heat capacity and Henry's constant (Equation 3-8) submodels are empirical, and typically only use two or three parameters of the between five and eleven available parameters. Models for C_p are shown in Table 3-1, but are not shown with the other equations below because several different model forms are available. Regression data are proprietary and are omitted.

Equation 3-9 is a form of the teenage vapor-liquid equilibrium equation (i.e., an intermediate for of the VLE that is usually adequate for engineering design), where the activity coefficient is referenced to the infinite dilution activity coefficient. Similarly, the henry's constant replaces the vapor pressure of component i in the solvent (water), because the Henry's constant is conceptualized as the constant of direct proportionality between vapor-phase partial pressure of component i and liquid phase mol fraction of i ($H=P_i/x_i$). This is only valid at ~infinite dilution of component i, but by an abuse of theory Equation 3-9 is serviceable. That is, γ^* is allowed to compensate for H, even though the activity coefficient is theoretically rooted in liquid-liquid non-idealities while Henry's constant is only valid at infinite dilution because of liquid non-idealities, but is conceptualized for largely non-condensable gases rather than all non-water components in a system. This abuse is a convenience introduced because much of the data and a number of submodels were referenced to the infinite dilution state, and Aspen does not have another convenient way to compensate for the change in reference state [2].

Finally, the location of the ionic activity coefficient τ parameters are given in Table 3-2, and Equations 3-10 through 3-13 show the equilibrium equation and the chemical equations used in Independence.

$$ln\left(H_{i,solvent}\right) = A_i + \frac{B_i}{T} + C_i ln(T) + D_i + \frac{E_i}{T^2} \quad \textbf{3-17}$$

$$y_i \phi_i P = x_i \gamma_i^* H_{i,H_2O} \quad \textbf{3-18}$$

$$-RTln\left(K_{eq}\right) = \frac{\Delta G^o}{RT} = \frac{\Delta G_0^o - \Delta H_0^o}{RT_0} + \frac{\Delta H_0^o}{RT} + \frac{1}{T}\int_{T_0}^{T} \frac{\Delta C_p^o}{R} dT - \int_{T_0}^{T} \frac{\Delta C_p^o}{RT} dT \quad \textbf{3-19}$$

$$2PZ + CO_2 \leftrightarrow PZH^+ + PZCOO^- \quad \textbf{3-20}$$

$$2PZCOO^- + CO_2 \leftrightarrow PZ(COO)_2^{2-} + H^+PZCOO^- \quad \textbf{3-21}$$

$$PZ + H^+PZCOO^- \leftrightarrow PZH^+ + PZCOO^- \quad \textbf{3-22}$$

Table 3-1 – Thermodynamic parameters of interest in Independence

Parameter Number	Parameter Location	Parameter Element	Parameter Designation	Parameter Description	Relevant equation
1	Properties>Methods>Parameters>Pure Components>CPAQ0	1	C1	This parameter Is in the heat capacity equation referenced to the infinite dilution in water state for CO3-	Cp=C1+C2*T+C3*T^2+C4/T+C5/T^2+C6/T^0.5
2	Properties>Methods>Parameters>Pure Components>CPAQ0	2	C2	This parameter Is in the heat capacity equation referenced to the infinite dilution in water state for CO3-	Cp=C1+C2*T+C3*T^2+C4/T+C5/T^2+C6/T^0.5
3	Properties>Methods>Parameters>Pure Components>CPAQ0	3	C3	This parameter Is in the heat capacity equation referenced to the infinite dilution in water state for CO3-	Cp=C1+C2*T+C3*T^2+C4/T+C5/T^2+C6/T^0.5

4	Properties>Methods>Parameters>Pure Components>CPAQ0	1	C1	This parameter Is in the heat capacity equation referenced to the infinite dilution in water state for HCO3-	Cp=C1+C2*T+C3*T^2+C4/T+C5/T^2+C6/T^0.5
5	Properties>Methods>Parameters>Pure Components>CPAQ0	2	C2	This parameter Is in the heat capacity equation referenced to the infinite dilution in water state for HCO3-	Cp=C1+C2*T+C3*T^2+C4/T+C5/T^2+C6/T^0.5
6	Properties>Methods>Parameters>Pure Components>CPAQ0	3	C3	This parameter Is in the heat capacity equation referenced to the infinite dilution in water state for HCO3-	Cp=C1+C2*T+C3*T^2+C4/T+C5/T^2+C6/T^0.5
7	Properties>Methods>Parameters>Pure Components>CPAQ0	1	C1	This parameter Is in the heat capacity equation referenced to the infinite dilution in water state for PZCOO-2	Cp=C1+C2*T+C3*T^2+C4/T+C5/T^2+C6/T^0.5
8	Properties>Methods>Parameters>Pure Components>CPAQ0	2	C2	This parameter Is in the heat capacity equation referenced to the infinite dilution in water state for PZCOO-2	Cp=C1+C2*T+C3*T^2+C4/T+C5/T^2+C6/T^0.5
9	Properties>Methods>Parameters>Pure Components>CPAQ0	1	C1	This parameter Is in the heat capacity equation referenced to the infinite dilution in water state for PZCOO-	Cp=C1+C2*T+C3*T^2+C4/T+C5/T^2+C6/T^0.5

10	Properties>Methods>Parameters>Pure Components>CPAQ0	2	C2	This parameter Is in the heat capacity equation referenced to the infinite dilution in water state for PZCOO-	Cp=C1+C2*T+C3*T^2+C4/T+C5/T^2+C6/T^0.5
11	Properties>Methods>Parameters>Pure Components>CPAQ0	1	C1	This parameter Is in the heat capacity equation referenced to the infinite dilution in water state for PZH+	Cp=C1+C2*T+C3*T^2+C4/T+C5/T^2+C6/T^0.5
12	Properties>Methods>Parameters>Pure Components>CPAQ0	2	C2	This parameter Is in the heat capacity equation referenced to the infinite dilution in water state for PZH+	Cp=C1+C2*T+C3*T^2+C4/T+C5/T^2+C6/T^0.5
13	Properties>Methods>Parameters>Pure Components>CPAQ0	1	C1	This parameter Is in the heat capacity equation referenced to the infinite dilution in water state for HPZCOO	Cp=C1+C2*T+C3*T^2+C4/T+C5/T^2+C6/T^0.5
14	Properties>Methods>Parameters>Pure Components>CPAQ0	2	C2	This parameter Is in the heat capacity equation referenced to the infinite dilution in water state for HPZCOO	Cp=C1+C2*T+C3*T^2+C4/T+C5/T^2+C6/T^0.5
15	Properties>Methods>Parameters>Pure Components>CPAQ0	1	C1	This parameter Is in the heat capacity equation referenced to the infinite dilution in water state for C5H14-01	Cp=C1+C2*T+C3*T^2+C4/T+C5/T^2+C6/T^0.5

16	Properties>Methods>Parameters>Pure Components>CPDIEC	1	A_B	This parameter is in the correlation for the dielectric constant of PZ	epsilon(T)=A_B+B_B*(1/T-1/C_B)
17	Properties>Methods>Parameters>Pure Components>CPDIEC	2	B_B	This parameter is in the correlation for the dielectric constant of PZ	epsilon(T)=A_B+B_B*(1/T-1/C_B)
18	Properties>Methods>Parameters>Pure Components>CPDIEC	3	C_B	This parameter is in the correlation for the dielectric constant of PZ	epsilon(T)=A_B+B_B*(1/T-1/C_B)
19	Properties>Methods>Parameters>Pure Components>CPIG	1	C_1	This parameter is in the correlation for Ideal gas heat capacity for HPZCOO	CP_IG(T)=C_1+C_2*T+C_3*T^2+C_4*T^3+C_5*T^4+C_6*T^5
20	Properties>Methods>Parameters>Pure Components>CPIG	2	C_2	This parameter is in the correlation for Ideal gas heat capacity for HPZCOO	CP_IG(T)=C_1+C_2*T+C_3*T^2+C_4*T^3+C_5*T^4+C_6*T^5
21	Properties>Methods>Parameters>Pure Components>CPIG	9	C_9	This parameter is in the correlation for Ideal gas heat capacity for HPZCOO for extrapolation below temperatures at C_7	CP_IG(T)=C_9+C_10*T
22	Properties>Methods>Parameters>Pure Components>CPIG	10	C_10	This parameter is in the correlation for Ideal gas heat capacity for HPZCOO for	CP_IG(T)=C_9+C_10*T^C_11

				extrapolation below temperatures at C_7	
23	Properties>Methods>Parameters>Pure Components>CPIG	11	C_11	This parameter is in the correlation for Ideal gas heat capacity for HPZCOO for extrapolation below temperatures at C_7	CP_IG(T)=C_9+C_10*T^C_11
24	Properties>Methods>Parameters>Pure Components>CPIG	7	C_7	This parameter is the lower temperature limit in the correlation for Ideal gas heat capacity for HPZCOO	N/A
25	Properties>Methods>Parameters>Pure Components>CPIG	1	C_1	This parameter is in the correlation for Ideal gas heat capacity (probably the Aspen polynomial) for PZ but not used because the DIPPR equation is indicated in THRSWT/7 and parameters for that are assigned in CPIGDP.	CP_IG(T)=C_1+C_2*T+C_3*T^2+C_4*T^3+C_5*T^4+C_6*T^5
26	Properties>Methods>Parameters>Pure Components>CPIG	2	C_2	This parameter is in the correlation for Ideal gas heat capacity (probably the Aspen polynomial) for PZ but not used because the	CP_IG(T)=C_1+C_2*T+C_3*T^2+C_4*T^3+C_5*T^4+C_6*T^5

				DIPPR equation is indicated in THRSWT/7 and parameters for that are assigned in CPIGDP.	
27	Properties>Methods>Parameters>Pure Components>CPIG	1	C_1	This parameter is in the correlation for Ideal gas heat capacity (probably the Aspen polynomial) for C5H13-01 but not used because the DIPPR equation is indicated in THRSWT/7 and parameters for that are assigned in CPIGDP.	CP_IG(T)=C_1+C_2*T+C_3*T^2+C_4*T^3+C_5*T^4+C_6*T^5
28	Properties>Methods>Parameters>Pure Components>CPIG	2	C_2	This parameter is in the correlation for Ideal gas heat capacity (probably the Aspen polynomial) for C5H13-01 but not used because the DIPPR equation is indicated in THRSWT/7 and parameters for that are assigned in CPIGDP.	CP_IG(T)=C_1+C_2*T+C_3*T^2+C_4*T^3+C_5*T^4+C_6*T^5
29	Properties>Methods>Parameters>Pure Components>CPIGDP	1	C_1	This parameter is in the correlation for Ideal gas heat capacity for C5H13-01 given that THRSWT/7=107 and the	CP_IG(T)=C_1+C_2*((C_3/T)/sinh(C_3/T))^2+C_4*((C_5/T_/cosh(C_5/T))

				parameters came from CPIGDP.	
30	Properties>Methods>Parameters>Pure Components>CPIGDP	2	C_2	This parameter is in the correlation for Ideal gas heat capacity for C5H13-01 given that THRSWT/7=107 and the parameters came from CPIGDP.	CP_IG(T)=C_1+C_2*((C_3/T)/sinh(C_3/T))^2+C_4*((C_5/T_/cosh(C_5/T))
31	Properties>Methods>Parameters>Pure Components>CPIGDP	3	C_3	This parameter is in the correlation for Ideal gas heat capacity for C5H13-01 given that THRSWT/7=107 and the parameters came from CPIGDP.	CP_IG(T)=C_1+C_2*((C_3/T)/sinh(C_3/T))^2+C_4*((C_5/T_/cosh(C_5/T))
32	Properties>Methods>Parameters>Pure Components>CPIGDP	4	C_4	This parameter is in the correlation for Ideal gas heat capacity for C5H13-01 given that THRSWT/7=107 and the parameters came from CPIGDP.	CP_IG(T)=C_1+C_2*((C_3/T)/sinh(C_3/T))^2+C_4*((C_5/T_/cosh(C_5/T))
33	Properties>Methods>Parameters>Pure Components>CPIGDP	5	C_5	This parameter is in the correlation for Ideal gas heat capacity for C5H13-01 given that THRSWT/7=107	CP_IG(T)=C_1+C_2*((C_3/T)/sinh(C_3/T))^2+C_4*((C_5/T_/cosh(C_5/T))

				and the parameters came from CPIGDP.	
34	Properties>Methods>Parameters>Pure Components>DHVLDP	1	C_1	This parameter uses the DIPPR equation (THRSWT/4=106) for the heat of vaporization of liquid PZ.	DelH_vap=C_1*(1-T_r)^(C_2+C_3*T+C_4*T^2+C_5*T^3)
35	Properties>Methods>Parameters>Pure Components>DHVLDP	2	C_2	This parameter uses the DIPPR equation (THRSWT/4=106) for the heat of vaporization of liquid PZ.	DelH_vap=C_1*(1-T_r)^(C_2+C_3*T+C_4*T^2+C_5*T^3)
36	Properties>Methods>Parameters>Pure Components>DHVLDP	3	C_3	This parameter uses the DIPPR equation (THRSWT/4=106) for the heat of vaporization of liquid PZ.	DelH_vap=C_1*(1-T_r)^(C_2+C_3*T+C_4*T^2+C_5*T^3)
37	Properties>Methods>Parameters>Pure Components>DHVLWT	1	C_1	This parameter uses the Watson equation (THRSWT/4=0) for the heat of vaporization of liquid H2O.	DelH_vap(T)=DelH_vap(T1)*((1-T/Tc)/(1_T1/Tc))^(a+b*(1-T/Tc))
38	Properties>Methods>Parameters>Pure Components>DHVLWT	2	C_2	This parameter uses the Watson equation (THRSWT/4=0) for the heat of vaporization of liquid H2O.	DelH_vap(T)=DelH_vap(T1)*((1-T/Tc)/(1_T1/Tc))^(a+b*(1-T/Tc))
39	Properties>Methods>Parameters>Pure	3	C_3	This parameter uses the Watson equation	DelH_vap(T)=DelH_vap(T1)*((1-

	Components> DHVLWT			(THRSWT/4=0) for the heat of vaporization of liquid H2O.	T/Tc)/(1_T1/Tc))^(a+ b*(1-T/Tc))
40	Properties>M ethods>Para meters>Pure Components> DHVLWT	4	C_4	This parameter uses the Watson equation (THRSWT/4=0) for the heat of vaporization of liquid H2O.	DelH_vap(T)=DelH_ vap(T1)*((1- T/Tc)/(1_T1/Tc))^(a+ b*(1-T/Tc))
41	Properties>M ethods>Para meters>Pure Components> DHVLWT	5	C_5	This parameter uses the Watson equation (THRSWT/4=0) for the heat of vaporization of liquid H2O.	DelH_vap(T)=DelH_ vap(T1)*((1- T/Tc)/(1_T1/Tc))^(a+ b*(1-T/Tc))
42	Properties>M ethods>Para meters>Pure Components> DNLDIP	1	A	This parameter uses the DIPPR equation 116 (THRSWT/2=116), typically used for H2O, for the liquid molar density of C5H13-01	kmol/cum=A+B*T^0 .35+C*T^(2/3)+D*T+ E*T^(4/3)
43	Properties>M ethods>Para meters>Pure Components> DNLDIP	2	B	This parameter uses the DIPPR equation 116 (THRSWT/2=116), typically used for H2O, for the liquid molar density of C5H13-01	kmol/cum=A+B*T^0 .35+C*T^(2/3)+D*T+ E*T^(4/3)
44	Properties>M ethods>Para meters>Pure Components> DNLDIP	3	C	This parameter uses the DIPPR equation 116 (THRSWT/2=116), typically used for H2O, for the liquid molar	kmol/cum=A+B*T^0 .35+C*T^(2/3)+D*T+ E*T^(4/3)

				density of C5H13-01	
45	Properties>Methods>Parameters>Pure Components>DNLDIP	4	D	This parameter uses the DIPPR equation 116 (THRSWT/2=116), typically used for H2O, for the liquid molar density of C5H13-01	kmol/cum=A+B*T^0.35+C*T^(2/3)+D*T+E*T^(4/3)
46	Properties>Methods>Parameters>Pure Components>IONMOB	1	see help	These are coefficients for PZH+ for the Jones-Dole correction to the viscosity of a solution due to the presence of electrolytes.	complicated and ugly, see help page
47	Properties>Methods>Parameters>Pure Components>IONMOB	2	see help	These are coefficients for PZH+ for the Jones-Dole correction to the viscosity of a solution due to the presence of electrolytes.	complicated and ugly, see help page
48	Properties>Methods>Parameters>Pure Components>IONMOB	1	see help	These are coefficients for PZCOO- for the Jones-Dole correction to the viscosity of a solution due to the presence of electrolytes.	complicated and ugly, see help page
49	Properties>Methods>Parameters>Pure	2	see help	These are coefficients for PZCOO- for the Jones-Dole	complicated and ugly, see help page

	Components>IONMOB			correction to the viscosity of a solution due to the presence of electrolytes.	
50	Properties>Methods>Parameters>Pure Components>IONMOB	1	see help	These are coefficients for PZCOO-2 for the Jones-Dole correction to the viscosity of a solution due to the presence of electrolytes.	complicated and ugly, see help page
51	Properties>Methods>Parameters>Pure Components>IONMOB	2	see help	These are coefficients for PZCOO-2 for the Jones-Dole correction to the viscosity of a solution due to the presence of electrolytes.	complicated and ugly, see help page
52	Properties>Methods>Parameters>Pure Components>MDH		see help	This is a parameter for the a Rackett equation mixing rule for PZ (to determine liquid molar volume). The parameter is VCRKT, which is the critical volume.	complicated and ugly, see help page
53	Properties>Methods>Parameters>Pure Components>MDH		see help	This is a parameter for the a Rackett equation mixing rule for PZ (to determine liquid molar volume). The parameter is RKTZRA, which appears to be the	complicated and ugly, see help page

				compressibility factor.	
54	Properties>Methods>Parameters>Pure Components>MDH		see help	This is a parameter for the a Rackett equation mixing rule for CO2 (to determine liquid molar volume). The parameter is RKTZRA, which appears to be the compressibility factor.	complicated and ugly, see help page
55	Properties>Methods>Parameters>Pure Components>MDH		see help	This is a parameter for the a Rackett equation mixing rule for CO2 (to determine liquid molar volume). The parameter is VCRKT, which is the critical volume.	complicated and ugly, see help page
56	Properties>Methods>Parameters>Pure Components>MDH		see help	This is a parameter for the a Rackett equation mixing rule for HPZCOO (to determine liquid molar volume). The parameter is VCRKT, which is the critical volume.	complicated and ugly, see help page
57	Properties>Methods>Parameters>Pure		see help	This is a parameter for the a Rackett equation mixing	complicated and ugly, see help page

	Components>MDH			rule for HPZCOO (to determine liquid molar volume). The parameter is RKTZRA, which appears to be the compressibility factor.	
58	Properties>Methods>Parameters>Pure Components>MDH		see help	This is a parameter for the a Rackett equation mixing rule for C5H13-01 (to determine liquid molar volume). The parameter is VCRKT, which appears to be the compressibility factor.	complicated and ugly, see help page
59	Properties>Methods>Parameters>Pure Components>MDH		see help	This is a parameter for the a Rackett equation mixing rule for C5H13-01 (to determine liquid molar volume). The parameter is RKTZRA, which appears to be the compressibility factor.	complicated and ugly, see help page
60	Properties>Methods>Parameters>Pure Components>Review	scalar	scalar	The aqueous gibbs energy of formation for C5H14-01.	scalar
61	Properties>Methods>Parameters>Pure	scalar	scalar	The aqueous enthalpy of formation for C5H14-01.	scalar

	Components> Review				
62	Properties>Methods>Parameters>Pure Components> USRDEF	scalar	scalar	The aqueous gibbs energy of formation for PZCOO-2	scalar
63	Properties>Methods>Parameters>Pure Components> USRDEF	scalar	scalar	The aqueous gibbs energy of formation for PZCOO-	scalar
64	Properties>Methods>Parameters>Pure Components> USRDEF	scalar	scalar	The aqueous gibbs energy of formation for HPZCOO	scalar
65	Properties>Methods>Parameters>Pure Components> USRDEF	scalar	scalar	The aqueous enthalpy of formation for PZCOO-2	scalar
66	Properties>Methods>Parameters>Pure Components> USRDEF	scalar	scalar	The aqueous enthalpy of formation for PZCOO-	scalar
67	Properties>Methods>Parameters>Pure Components> USRDEF	scalar	scalar	The aqueous enthalpy of formation for HPZCOO	scalar
68	Properties>Methods>Parameters>Pure Components> USRDEF	scalar	scalar	The gibbs energy of formation for HPZCOO	scalar
69	Properties>Methods>Parameters>Pure	scalar	scalar	The enthalpy of formation for HPZCOO	scalar

	Components>USRDEF				
70	Properties>Methods>Parameters>Binary Interaction>Henry	1	AIJ	All molecular species were declared as Henry's components (except water, which is the solvent). This is a parameter in the Henry's law correlation for PZ.	H_i,j=AIJ+BIJ/T+CIJ*ln(T)+DIJ*T+EIJ/T^2
71	Properties>Methods>Parameters>Binary Interaction>Henry	2	BIJ	All molecular species were declared as Henry's components (except water, which is the solvent). This is a parameter in the Henry's law correlation for PZ.	H_i,j=AIJ+BIJ/T+CIJ*ln(T)+DIJ*T+EIJ/T^2
72	Properties>Methods>Parameters>Binary Interaction>Henry	3	CIJ	All molecular species were declared as Henry's components (except water, which is the solvent). This is a parameter in the Henry's law correlation for PZ.	H_i,j=AIJ+BIJ/T+CIJ*ln(T)+DIJ*T+EIJ/T^2
73	Properties>Methods>Parameters>Binary Interaction>Henry	4	DIJ	All molecular species were declared as Henry's components (except water, which is the solvent). This is a parameter in the	H_i,j=AIJ+BIJ/T+CIJ*ln(T)+DIJ*T+EIJ/T^2

				Henry's law correlation for PZ.	
74	Properties>Methods>Parameters>Binary Interaction>Henry	1	AIJ	All molecular species were declared as Henry's components (except water, which is the solvent). This is a parameter in the Henry's law correlation for C5H13-01.	H_i,j=AIJ+BIJ/T+CIJ*ln(T)+DIJ*T+EIJ/T^2
75	Properties>Methods>Parameters>Binary Interaction>Henry	2	BIJ	All molecular species were declared as Henry's components (except water, which is the solvent). This is a parameter in the Henry's law correlation for C5H13-01.	H_i,j=AIJ+BIJ/T+CIJ*ln(T)+DIJ*T+EIJ/T^2
76	Properties>Methods>Parameters>Binary Interaction>Henry	3	CIJ	All molecular species were declared as Henry's components (except water, which is the solvent). This is a parameter in the Henry's law correlation for C5H13-01.	H_i,j=AIJ+BIJ/T+CIJ*ln(T)+DIJ*T+EIJ/T^2
77	Properties>Methods>Parameters>Binar	4	DIJ	All molecular species were declared as	H_i,j=AIJ+BIJ/T+CIJ*ln(T)+DIJ*T+EIJ/T^2

	y Interaction>Henry			Henry's components (except water, which is the solvent). This is a parameter in the Henry's law correlation for C5H13-01.	
78	Properties>Methods>Parameters>Binary Interaction>NRTL-1	1	AJI	This parameter is used for computing tau for the molecule-molecule portion of the NRTL model. Component I is water and J is PZ.	tau_i,j=AIJ+BIJ/T+EIJ*ln(T)+FIJ*T
79	Properties>Methods>Parameters>Binary Interaction>NRTL-1	2	BJI	This parameter is used for computing tau for the molecule-molecule portion of the NRTL model. Component I is water and J is PZ.	tau_i,j=AIJ+BIJ/T+EIJ*ln(T)+FIJ*T
80	Properties>Methods>Parameters>Binary Interaction>NRTL-1	1	AIJ	This parameter is used for computing tau for the molecule-molecule portion of the NRTL model. Component I is HPZCOO and J is CO2.	tau_i,j=AIJ+BIJ/T+EIJ*ln(T)+FIJ*T
81	Properties>Methods>Parameters>Binary Interaction>NRTL-1	2	BIJ	This parameter is used for computing tau for the molecule-molecule portion of the NRTL model.	tau_i,j=AIJ+BIJ/T+EIJ*ln(T)+FIJ*T

				Component I is HPZCOO and J is CO2.	
82	Properties>Methods>Parameters>Binary Interaction>NRTL-1	1	AJI	This parameter is used for computing tau for the molecule-molecule portion of the NRTL model. Component I is CO2 and J is PZ.	tau_i,j=AIJ+BIJ/T+EIJ*ln(T)+FIJ*T
83	Properties>Methods>Parameters>Binary Interaction>NRTL-1	2	BJI	This parameter is used for computing tau for the molecule-molecule portion of the NRTL model. Component I is CO2 and J is PZ.	tau_i,j=AIJ+BIJ/T+EIJ*ln(T)+FIJ*T
84	Properties>Methods>Parameters>Binary Interaction>NRTL-1	1	AJI	This parameter is used for computing tau for the molecule-molecule portion of the NRTL model. Component I is H2O and J is C5H13-01.	tau_i,j=AIJ+BIJ/T+EIJ*ln(T)+FIJ*T
85	Properties>Methods>Parameters>Binary Interaction>NRTL-1	2	BJI	This parameter is used for computing tau for the molecule-molecule portion of the NRTL model. Component I is H2O and J is C5H13-01.	tau_i,j=AIJ+BIJ/T+EIJ*ln(T)+FIJ*T

86	Properties>Methods>Parameters>Binary Interaction>NRTL-1	1	AIJ	This parameter is used for computing tau for the molecule-molecule portion of the NRTL model. Component I is C5H13-01 and J is CO2.	tau_i,j=AIJ+BIJ/T+EIJ*ln(T)+FIJ*T
87	Properties>Methods>Parameters>Binary Interaction>NRTL-1	2	BIJ	This parameter is used for computing tau for the molecule-molecule portion of the NRTL model. Component I is C5H13-01 and J is CO2.	tau_i,j=AIJ+BIJ/T+EIJ*ln(T)+FIJ*T
88	Properties>Methods>Parameters>Binary Interaction>NRTL-1	1	AJI	This parameter is used for computing tau for the molecule-molecule portion of the NRTL model. Component I is C5H13-01 and J is CO2.	tau_i,j=AIJ+BIJ/T+EIJ*ln(T)+FIJ*T
89	Properties>Methods>Parameters>Binary Interaction>NRTL-1	2	BJI	This parameter is used for computing tau for the molecule-molecule portion of the NRTL model. Component I is C5H13-01 and J is CO2.	tau_i,j=AIJ+BIJ/T+EIJ*ln(T)+FIJ*T

90	Properties>Methods>Parameters>Binary Interaction>NRTL-1	3	CIJ	This parameter is typically computed via a heuristic, and is used to compute alpha, which appears to be symmetrical in this case. Component I is H2O and component J is PZ.	alpha_i,j=CIJ+(T-273.15)*DIJ
91	Properties>Methods>Parameters>Binary Interaction>NRTL-1	3	CIJ	This parameter is typically computed via a heuristic, and is used to compute alpha, which appears to be symmetrical in this case. Component I is HPZCOO and component J is CO2.	alpha_i,j=CIJ+(T-273.15)*DIJ
92	Properties>Methods>Parameters>Binary Interaction>NRTL-1	3	CIJ	This parameter is typically computed via a heuristic, and is used to compute alpha, which appears to be symmetrical in this case. Component I is CO2 and component J is PZ.	alpha_i,j=CIJ+(T-273.15)*DIJ
93	Properties>Methods>Parameters>Binary	3	CIJ	This parameter is typically computed via a heuristic, and is used to compute	alpha_i,j=CIJ+(T-273.15)*DIJ

	Interaction>NRTL-1			alpha, which appears to be symmetrical in this case. Component I is H2O and component J is C5H13-01.	
94	Properties>Methods>Parameters>Binary Interaction>NRTL-1	3	CIJ	This parameter is typically computed via a heuristic, and is used to compute alpha, which appears to be symmetrical in this case. Component I is C5H13-01 and component J is CO2.	alpha_i,j=CIJ+(T-273.15)*DIJ
95	Properties>Methods>Parameters>Binary Interaction>NRTL-1	3	CIJ	This parameter is typically computed via a heuristic, and is used to compute alpha, which appears to be symmetrical in this case. Component I is PZ and component J is C5H13-01.	alpha_i,j=CIJ+(T-273.15)*DIJ
96	Properties>Methods>Parameters>Binary Interaction>NRTL-1	3	CIJ	This parameter is typically computed via a heuristic, and is used to compute alpha, which appears to be symmetrical in this case. Component I is C5H13-01 and	alpha_i,j=CIJ+(T-273.15)*DIJ

				component J is HPZCOO.	
97	Properties>Methods>Parameters>Binary Interaction>VLCLK	1	VCA	This parameter is used to calculate the liquid molar volume using the Clarke equation for electrolyte solutions of PZH+ and PZCOO-	Messy, see help pages.
98	Properties>Methods>Parameters>Binary Interaction>VLCLK	2	ACA	This parameter is used to calculate the liquid molar volume using the Clarke equation for electrolyte solutions of PZH+ and PZCOO-	Messy, see help pages.
99	Properties>Methods>Parameters>Binary Interaction>VLCLK	1	VCA	This parameter is used to calculate the liquid molar volume using the Clarke equation for electrolyte solutions of PZH+ and HCO3-	Messy, see help pages.
100	Properties>Methods>Parameters>Binary Interaction>VLCLK	2	ACA	This parameter is used to calculate the liquid molar volume using the Clarke equation for electrolyte solutions of PZH+ and HCO3-	Messy, see help pages.
101	Properties>Methods>Parameters>Binary Interaction>VLCLK	1	VCA	This parameter is used to calculate the liquid molar volume using the Clarke equation for electrolyte	Messy, see help pages.

				solutions of PZH+ and PZCOO-2	
102	Properties>Methods>Parameters>Binary Interaction>VLCLK	2	ACA	This parameter is used to calculate the liquid molar volume using the Clarke equation for electrolyte solutions of PZH+ and PZCOO-2	Messy, see help pages.
103	Properties>Methods>Parameters>Binary Interaction>VLCLK	1	VCA	This parameter is used to calculate the liquid molar volume using the Clarke equation for electrolyte solutions of C5H14-01 and HCO3-	Messy, see help pages.
104	Properties>Methods>Parameters>Binary Interaction>VLCLK	2	ACA	This parameter is used to calculate the liquid molar volume using the Clarke equation for electrolyte solutions of C5H14-01 and HCO3-	Messy, see help pages.
105	Properties>Methods>Parameters>Binary Interaction>VLCLK	1	VCA	This parameter is used to calculate the liquid molar volume using the Clarke equation for electrolyte solutions of C5H14-01 and CO3-2	Messy, see help pages.
106	Properties>Methods>Parameters>Binary	2	ACA	This parameter is used to calculate the liquid molar volume using the Clarke equation	Messy, see help pages.

	Interaction>VLCLK			for electrolyte solutions of C5H14-01 and CO3-2	

Table 3-2 – Ionic τ values[2]

Location	$\tau_{m,ca}$ or $\tau_{ca,m}$ "a" Values (GMEL-CC)
Properties>Methods>Parameters>Electrolyte Pair>GMEL-CC-1	H2O
	PZH+
	PZCOO-
"	PZH+
	PZCOO-
	H2O
"	PZ
	PZH+
	PZCOO-
"	PZH+
	PZCOO-
	PZ
"	PZH+
	PZCOO-

[2] The parameters in Table 3-2 have their greatest impact in the *difference* between each pair of molecule-ion interactions ($\tau_{m,ca}$ and $\tau_{ca,m}$). Therefore, only one parameter is adjusted (highlighted in blue) while the other half of the pairwise interaction is stationary (highlighted in red).

	HPZCOO
	PZH+
	HCO3-
“	HPZCOO
	HPZCOO
	PZH+
“	HCO3-
	HPZCOO
	PZH+
“	PZCOO-
	PZH+
	PZCOO-2
“	HPZCOO
	HPZCOO
	PZH+
“	PZCOO-2
	H2O
	PZH+
“	PZCOO-2
	PZH+
	PZCOO-2
“	H2O
	PZ
“	PZH+

	PZCOO-2
	PZH+
	PZCOO-2
"	PZ
	$\tau_{m,ca}$ or $\tau_{ca,m}$ "b" Values (GMEL-CD)
	PZH+
	PZCOO-
Properties>Methods>Parameters>Electrolyte Pair>GMEL-CD-1	CO2

Results

The size and complexity of the thermodynamic parameter set requires a multi-tier calibration. In this case, there is a first tier of parameters that propagate forward into the second tier of submodels. Tier 1 sample results are shown below, where red lines are the calibrated model prediction at the 95% confidence level, black lines are the calibrated model including discrepancy (also at the 95% confidence level), and black dots are data. Figure 3 show the calibrated heat capacity model, with excellent model/data agreement. Figure 4 demonstrates relatively poor agreement with large uncertainty, but this is a direct artefact of the data (which has wide scatter). It also recently became apparent that a high temperature data set was excluded from the Henry's constant calibration, which increases uncertainty considerably[3] for a model form that is exponential in temperature. Finally, Figure 5 shows the univariate (diagonal) and bivariate (off-diagonals) marginal posterior distributions for the τ and $H_{i,H2O}$ parameters. Note that the τ parameters were well defined by the calibration, and settled on a probability region consistent with past experience [15]. The Henry's constant parameters were not well defined in the

[3] In this case, the Henry's constant is found from a 5-parameter empirical correlation. If only the low temperature data is used, the correlation predicts the data reasonably well, and only needs to fit two parameters to do so. The allowable values of the remaining parameters (at a 95% joint confidence level) result in predictions that over or under predict reality by approximately an order of magnitude. When data in submodels fails to span the entire operating range, and extrapolations must be made, their impact on the uncertainty (and the effort that should be spent in filling the data gap) may be determined mathematically or by expert intuition. Rigorously, the mathematical option is superior, but within practical resource constraints, the expert intuition is usually relied upon.

univariate marginal, but the bivariate marginal of Henry's constant parameters one and two show that the model is relatively tightly defined when those parameters are conditioned on each other. The third Henry's constant parameter is not refined in any meaningful way either in the univariate or bivariate, which was expected in this case. The empirical model allows for up to five parameters (to span a large temperature range accurately). In this case, the temperature range is narrow, and only two parameters are useful in fitting the data, while the third parameter does not improve the fit, as can be noted from a simple regression of the linearized model.

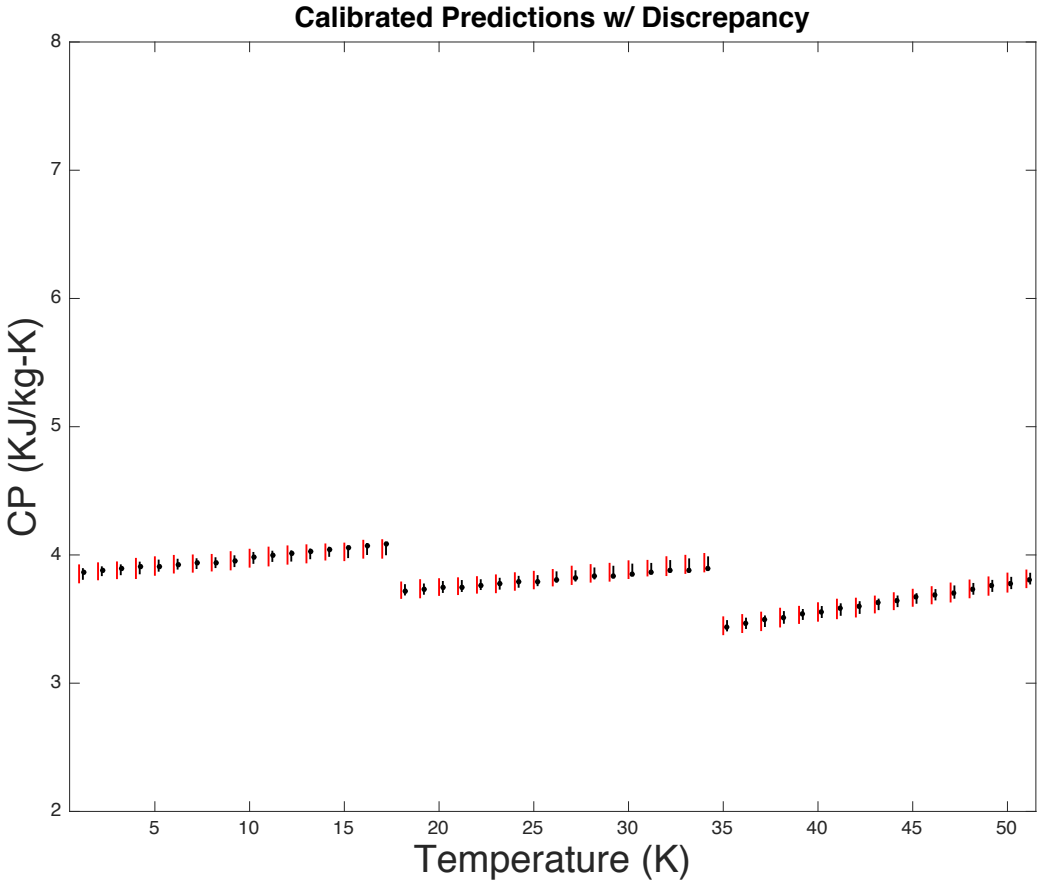

Figure 3 – Calibrated predictions of the heat capacity

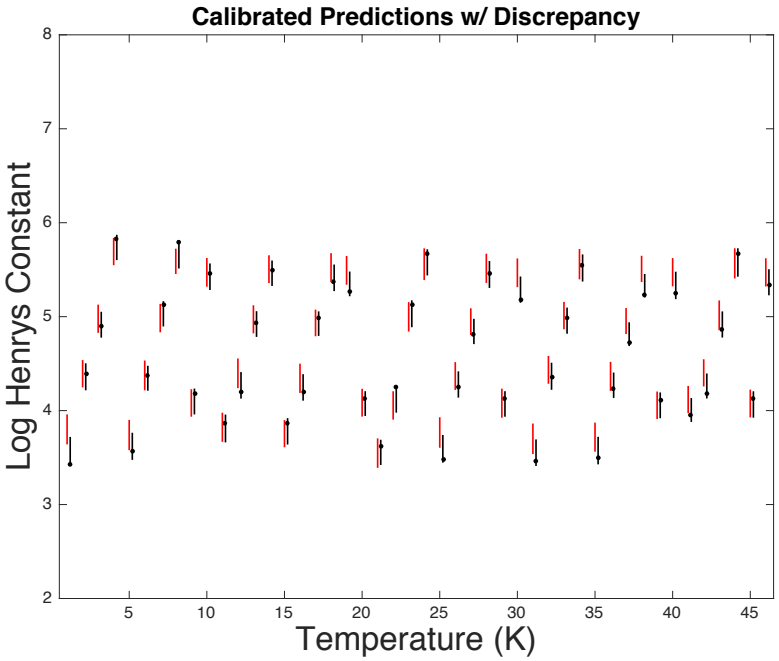

Figure 4 – Calibrated predictions of the Henry's constant

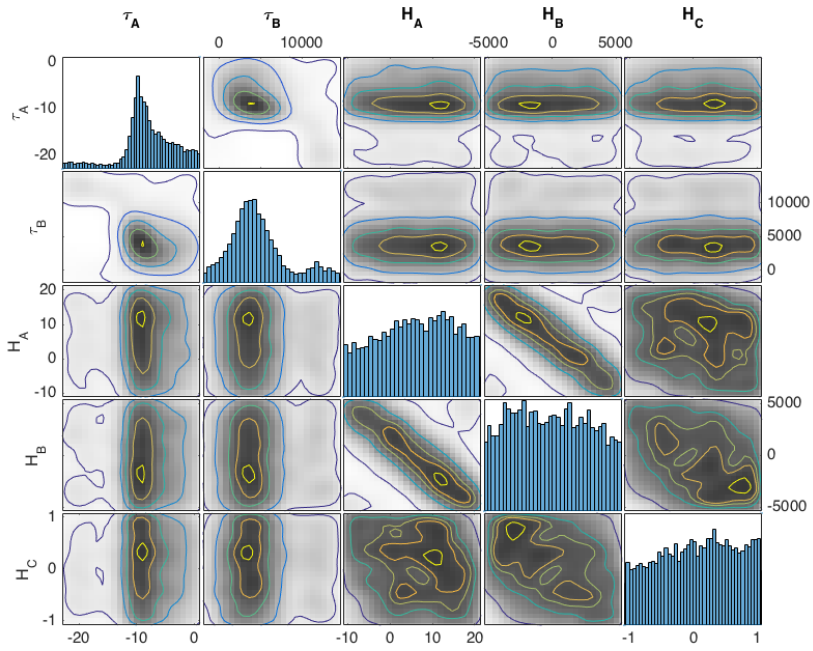

Figure 5 – Univariate and bivariate posterior marginal PDFs

4.0 Ongoing Work

Chemical process systems are complex networks of dozens or hundreds of thermodynamic, heat and mass transfer, and kinetic parameters, with additional parameters for the macro-scale process. The interactions and number of these parameters make proper emulation infeasible in a single step, and work is underway for hierarchical propagation of error, so that subsets of parameters and data can be calibrated separately, as shown in Figure 5.

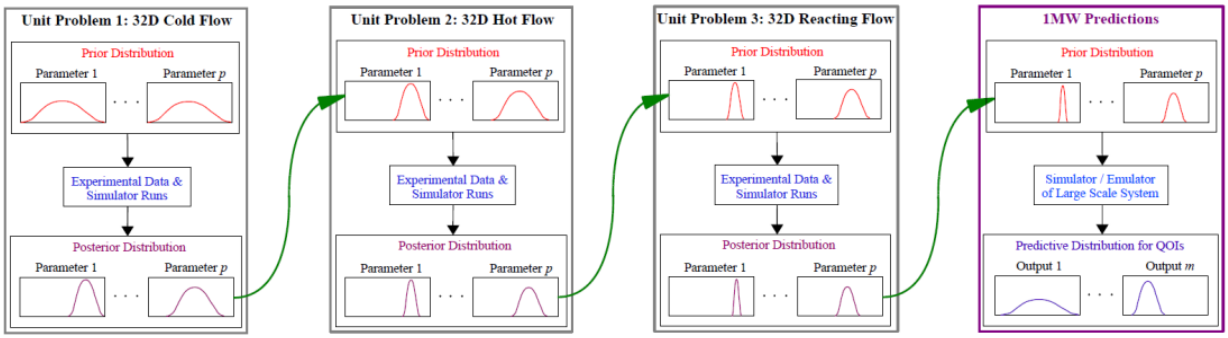

Figure 6 – Hierarchical calibration flow diagram

5.0 References

1. Holland, T. M. A Comprehensive Coal Conversion Model Extended to Oxy-coal Conditions. Ph. D thesis, Brigham Young University, Provo, UT, 2017.

2. Hilliard, M. D. A Predictive Thermodynamic Model for an Aqueous Blend of Potassium

Carbonate, Piperazine, and Monoethanolamine for Carbon Dioxide

Capture from Flue Gas. UT Austin, Austin, TX, 2008.

3. Nguyen, B.-T. N. Amine Volatility in CO2 Capture. UT Austin, Austin, TX, 2013.

4. Dugas, R. E. Carbon Dioxide Absorption, Desorption, and Diffusion in Aqueous

Piperazine and Monoethanolamine. UT Austin, Austin, TX, 2009.

5. Fulk, S. M. Measuring and Modeling Aerosols in Carbon Dioxide Capture by Aqueous Amines. UT Austin, Austin, Tx, 2016.

6. Xu, Q. Thermodynamics of CO2 Loaded Aqueous Amines. UT Austin, Austin, Tx, 2011.

7. Freeman, S. A. Thermal Degradation and Oxidation of Aqueous Piperazine

for Carbon Dioxide Capture. UT Austin, Austin, TX, 2011.

8. Morgan, J. C.; Bhattacharyya, D.; Tong, C.; Miller, D. C., Uncertainty quantification of property models: Methodology and its application to CO2-loaded aqueous MEA solutions. *AIChE Journal* **2015,** 61, (6), 1822-1839.

9. Welch, W. J.; Buck, R. J.; Sacks, J.; Wynn, H. P.; Mitchell, T. J.; Morris, M. D., SCREENING, PREDICTING, AND COMPUTER EXPERIMENTS. *Technometrics* **1992,** 34, (1), 15-25.

10. Sacks J., W., W.J., Mitchell, T.J. and Wynn, H.P. , *Statistical Science* **1989,** 4, 409-423.

11. Gattiker, J., Myers, K., Williams, B., Higdon, D., Carzolio, M., & Hoegh, A. , Gaussian Process-Based Sensitivity Analysis and Bayesian Model Calibration with GPMSA. In *Handbook of Uncertainty Quantification*, Ghanem, H., Owadhi, Ed. Springer: 2017; pp 1-41.

12. Gattiker, J.; Myers, K.; Higdon, D.; Williams, B., Handbook of Uncertainty Quantification. In Ghanem, H., Owadhi, Ed. Spring: New York, 2016.

13. Higdon, D.; Gattiker, J.; Williams, B.; Rightley, M., Computer model calibration using high-dimensional output. *Journal of the American Statistical Association* **2008,** 103, (482), 570-583.

14. Storlie, C. B.; Lane, W. A.; Ryan, E. M.; Gattiker, J. R.; Higdon, D. M., Calibration of Computational Models With Categorical Parameters and Correlated Outputs via Bayesian

Smoothing Spline ANOVA. *Journal of the American Statistical Association* **2015,** 110, (509), 68-82.

15. Frailie, P. Modeling of Carbon Dioxide Absorbing/Stripping by Aqueous Methyldiethanolamine/Piperazine. UT Austin, Austin, TX, 2014.